

Solar Flare Occurrence Rate and Probability in Terms of the Sunspot Classification Supplemented with Sunspot Area and Its Changes

Kangjin Lee · Y.-J. Moon · Jin-Yi Lee ·
Kyoung-Sun Lee · Hyeonock Na

Received: 19 December 2011 / Accepted: 25 July 2012 / Published online: 7 September 2012
© Springer Science+Business Media B.V. 2012

Abstract We investigate the solar flare occurrence rate and daily flare probability in terms of the sunspot classification supplemented with sunspot area and its changes. For this we use the NOAA active region data and GOES solar flare data for 15 years (from January 1996 to December 2010). We consider the most flare-productive 11 sunspot classes in the McIntosh sunspot group classification. Sunspot area and its changes can be a proxy of magnetic flux and its emergence/cancellation, respectively. We classify each sunspot group into two sub-groups by its area: “Large” and “Small”. In addition, for each group, we classify it into three sub-groups according to sunspot area changes: “Decrease”, “Steady”, and “Increase”. As a result, in the case of compact groups, their flare occurrence rates and daily flare probabilities noticeably increase with sunspot group area. We also find that the flare occurrence rates and daily flare probabilities for the “Increase” sub-groups are noticeably higher than those for the other sub-groups. In case of the (M + X)-class flares in the ‘Dkc’ group, the flare occurrence rate of the “Increase” sub-group is three times higher than that of the “Steady” sub-group. The mean flare occurrence rates and flare probabilities for all sunspot groups increase with the following order: “Decrease”, “Steady”, and “Increase”. Our results statistically demonstrate that magnetic flux and its emergence enhance the occurrence of major solar flares.

Keywords Flares, forecasting · Sunspots, statistics

K. Lee · Y.-J. Moon (✉) · H. Na
School of Space Research, Kyung Hee University, Yongin, Korea
e-mail: moonjy@khu.ac.kr

K. Lee
e-mail: canopus@khu.ac.kr

K. Lee
National Meteorological Satellite Center, Korea Meteorological Administration, Jincheon, Korea

Y.-J. Moon · J.-Y. Lee · K.-S. Lee
Astronomy & Space Science, Kyung Hee University, Yongin, Korea

1. Introduction

Solar flares explosively release a large amount of energy in the form of high energy particles and radiation from radio waves to gamma-rays. Since the electromagnetic waves from a flare site arrive at the Earth earlier than energetic protons (solar proton events, SPEs) and much earlier than coronal mass ejections (CMEs), it is very difficult to prepare for hazards by them. Soft X-ray enhancements due to large flares cause increased ionization of the upper atmosphere, which can cause short-wave radio fade-outs (Wheatland, 2005) and result in enormous economic and commercial losses (Baker, 2005). Thus, the forecast of solar flares becomes more important in modern age.

Most solar flares originate in active regions (ARs) including sunspot groups. In the past, three types of sunspot classification have been used to explain sunspot groups: Zurich classification, Mount Wilson magnetic classification, and McIntosh classification. The Zurich sunspot classification was developed by Walmeier (1947) by modifying an earlier scheme of classification introduced by Cortie (1901). While the McIntosh classification makes use of the size, stability, and complexity of sunspot groups (McIntosh, 1990), the Mount Wilson classification uses magnetic characteristics of sunspots (Hale *et al.*, 1919). The McIntosh classification provides a method for describing the properties of solar active regions based on white-light images (Bornmann, Kalmbach, and Kulhanek, 1994). There are three parameters in the McIntosh classification: Z, p, and c. Parameter Z represents the modified Zurich class (A, B, C, D, E, F, G, or H), which is defined on the basis of whether penumbra is present, how penumbra is distributed, and by the length of the group. Parameter p specifies the type of principal sunspot (x, r, s, a, h, or k), primarily describing its penumbra. Parameter c specifies the degree of compactness (x, o, i, or c) in the interior of the group. The logical sequence for determining the McIntosh sunspot types (60 in total) begins with the distinction of sunspots between unipolar and bipolar (McIntosh, 1990).

Currently, the solar flare forecasting schemes are classified into three types:

- i) morphological schemes,
- ii) statistical schemes, and
- iii) machine learning schemes.

Fundamentally, all three are based on morphological characteristic of sunspot groups. However, the first type of schemes (morphological schemes) uses only the morphological characteristics of sunspot groups. Specifically, these schemes make use of historical records of flare rates for each type of sunspot groups to estimate the flare occurrence rates and probabilities (McIntosh, 1990; Bornmann and Shaw, 1994; Gallagher, Moon, and Wang, 2002). The second type of schemes (statistical schemes) is based on the morphological schemes but relies on a statistical analysis of the flare-related sunspot properties and flare intensities by mathematical models (Wheatland 2004, 2005; Zharkov and Zharkova 2004, 2006; Barnes *et al.*, 2007; Yu *et al.*, 2009). For example, Barnes *et al.* (2007) investigated statistically the magnetic parameters having the best relationship with flare occurrence. The third type of schemes (machine learning schemes) is a branch of artificial intelligence which allows computers to evolve a model system based on empirical data such as the type of sunspot groups. Recently, machine learning schemes such as neural network were also employed for flare forecasting (Wang *et al.*, 2008; Colak and Qahwaji, 2008; Yuan *et al.*, 2010).

There are representative flare forecast models that are currently operated in National Oceanic and Atmospheric Administration (NOAA)/Space Weather Prediction Cen-

ter (SWPC)¹ and Active Region Monitor (ARM).² These models employ statistics of solar flares for given sunspot classes (e.g., by using the McIntosh sunspot group classification); therefore they are morphological schemes. These models have a good advantage that input data are easily obtained and routinely provided; Solar Region Summary (SRS) data are daily provided on the web. In this study, we consider additional two parameters: sunspot group area and its changes. The sunspot area can be a good proxy for the magnetic flux of a sunspot. Zharkov and Zharkova (2006) showed that the magnetic flux has a very good linear correlation with the sunspot area with the correlation coefficient of about 0.94. We note that the magnetic flux of an active region is related to the occurrence of flares from that region (Giovanelli, 1939; Greatrix, 1963; Veronig, Temmer, and Hanslmeier, 2004), and magnetic flux emergence is one of the important mechanisms for triggering solar flares (Heyvaerts, Priest, and Rust, 1977; Tur and Priest, 1978).

For this work, we adopt the sunspot group area and its changes as a proxy for the magnetic flux and degree of flux emergence/cancellation in the group. We also investigate daily mean flare occurrence rates and probabilities. For this, we use sunspot and flare data from NOAA from 1996 to 2010.

This paper is organized as follows. In Section 2, we describe the data and method of analysis. Results are shown in Section 3. Finally, summary and conclusions are presented in Section 4.

2. Data and Analysis

2.1. Data

In this study, we use two kinds of data set: data on active regions (ARs) and on solar flares. For the data on ARs, we use the numbers, areas, and McIntosh classes (McIntosh, 1990) of ARs in NOAA's SRS from January 1996 to December 2010.³ The characteristics for each AR are compiled from up to six observatories that report to the NOAA/SWPC in near real time. In the analysis, ARs are assigned the NOAA/United States Air Force (USAF) sunspot region numbers. The sunspot area used here is the total corrected area of a group in millionths of the solar hemisphere. The number of ARs which were assigned one of 60 McIntosh classes (allowing multiple counts if a single NOAA active region evolves through several classes) is 23 500. If an AR is observed for several days, we assign a sunspot group class to it on each day of observation (one NOAA region has multiple counts for several observed days). If we consider 11 sunspot group classes which are most productive as described below, the number of independent regions (one NOAA region number is only counted once) is 596 (see Section 2.2).

For the solar flare records, we use the data from National Geophysical Data Center (NGDC).⁴ The intensities of solar flares are measured by the *Geostationary Operational Environmental Satellite* (GOES). The X-ray flares are classified according to the order of magnitude of the peak intensity measured at the Earth in the wavelength band of 1 to 8 Å which

¹<http://www.swpc.noaa.gov/>.

²<http://www.solarmonitor.org/>.

³<http://www.swpc.noaa.gov/ftpmenu/warehouse.html>.

⁴ftp://ftp.ngdc.noaa.gov/STP/SOLAR_DATA/SOLAR_FLARES/FLARES_XRAY/.

was chosen because radiation at these wavelengths is largely responsible for the ionospheric disturbances which disrupt telecommunications (Kildahl, 1980). In this study, we use X-ray flares stronger than B-class; namely C, M, and X-class flares. The major flares such as M and X-class flares are mostly associated with CMEs (Andrews, 2003). The data we used include about 7400 C-class flares, 1200 M-class flares, and 100 X-class flares during the analyzed period. In this study, the number of X-class flares is relatively small. Therefore, we combine the M-class flares with the X-class flares, which is called “(M + X)-class” hereafter.

2.2. Selection of Sunspot Groups

We identify the McIntosh sunspot classes of all sunspot groups for 15 years and their associated GOES X-ray flares to determine their flare occurrence numbers and flare occurrence rates (the number of flares/the number of active regions). Table 1 shows the number of C-class solar flares and sunspot groups in all McIntosh sunspot groups. For example, ‘Axx’, ‘Bxo’, ‘Cao’, ‘Cso’, ‘Dao’, ‘Dso’, and ‘Hsx’ groups appear more frequently than the other groups. However, solar flares are highly productive in ‘Eki’, ‘Fki’, ‘Ekc’, and ‘Fkc’ groups. These characteristics are similar to Norquist (2011).

For the present study we use the McIntosh sunspot group classification with 11 flare-productive groups: ‘Dai’, ‘Eai’, ‘Fai’, ‘Dko’, ‘Eko’, ‘Dki’, ‘Dkc’, ‘Eki’, ‘Ekc’, ‘Fki’, and ‘Fkc’. These 11 sunspot groups satisfy the following conditions: the number of the (M + X)-class flares is more than 20 and the flare occurrence rate is higher than 0.1 (see Table 2).

2.3. Definition of Sub-Groups According to Areas and Area Changes of Sunspots

We investigate the relationship between solar flare occurrence and sunspot areas. According to the area of sunspot groups, we classify them into two sub-groups which have similar numbers in membership: “Large” and “Small”. For this, based on the area distribution of sunspot groups we selected the dividing value of the area. Several studies have shown that the magnetic flux of ARs is related to the sunspot areas (Giovannelli, 1939; Greatrix, 1963; Veronig, Temmer, and Hanslmeier, 2004). This result verifies that the sunspot area can be a good proxy for the AR magnetic flux. Therefore, in this study, we use the area changes of sunspot groups as a proxy of magnetic flux changes.

We classify each sunspot group into three sub-groups according to how the sunspot group area change (ΔA): “Decrease” ($\Delta A \leq -90$ m.i.h.), “Steady” (-90 m.i.h. $< \Delta A < 90$ m.i.h.), and “Increase” ($\Delta A \geq 90$ m.i.h.). Here 90 m.i.h. corresponds to the standard deviation of area change which is computed from a Gaussian fitting to the distribution of area changes.

2.4. Flare Occurrence Rate and Flare Probability

For calculating flare probability for each sunspot class, first we calculate its flare occurrence rate. For example, there are 222 regions classified ‘Fkc’ during the period. As this class produced 531 C-class events, the mean occurrence rate of C-class flares is $\approx 531/222$ or ≈ 2.39 flares per day (see Table 1). Next, we estimate its flare probability. Assuming the number of flares per unit time is governed by Poisson statistics, we estimate a flaring probability for the following 24 h. Wheatland (2000) showed that the waiting time distribution of flares is consistent with a time-dependent Poisson process and the probability of flare occurrence per unit time follows an approximate exponential distribution. Moon *et al.* (2001) also showed that the waiting time distribution of flares follows a Poisson probability function. The Poisson distribution is a discrete probability distribution that expresses the probability of a given

Table 1 The occurrence rates of C-class flares according to 60 McIntosh sunspot group classes. The numerator represents the number of flares observed in each class whose membership count is shown in the denominator.

Axx 80/2820	Bxo 224/3121	Bxi 0/7	Cro 80/764	Cri 3/5	Dro 38/172	Dri 8/9	Ero 0/5	Eri 0/0	Fro 0/1	Fri 0/0	Hrx 26/419
Cso 332/2415	Csi 3/10	Dso 461/1701	Dsi 57/109	Dsc 7/7	Eso 105/315	Esi 56/72	Esc 4/8	Fso 17/53	Fsi 27/20	Fsc 6/3	Hsx 175/3076
Cao 267/1282	Cai 20/27	Dao 763/2081	Dai 398/466	Dac 107/68	Eao 315/587	Eai 415/454	Eac 99/76	Fao 89/100	Fai 177/143	Fac 43/31	Hax 128/867
Cho 32/81	Chi 1/3	Dho 24/57	Dhi 7/12	Dhc 5/5	Eho 32/33	Ehi 39/30	Ehc 3/4	Fho 21/19	Fhi 13/10	Fhc 35/10	Hhx 20/102
Cko 49/139	Cki 10/8	Dko 114/187	Dki 226/178	Dkc 187/107	Eko 142/155	Eki 435/326	Ekc 511/230	Fko 61/70	Fki 352/184	Fkc 531/222	Hkx 28/101

Table 2 The occurrence rates of (M + X)-class flares according to 60 McIntosh sunspot group classes. The numerator represents the number of flares observed in each class whose membership count is shown in the denominator.

Axx 9/2820	Bxo 14/3121	Bxi 0/7	Cro 6/764	Cri 0/5	Dro 2/172	Dri 0/9	Ero 0/5	Eri 0/0	Fro 0/1	Fri 0/0	Hrx 1/419
Cso 42/2415	Csi 0/10	Dso 34/1701	Dsi 6/109	Dsc 0/7	Eso 7/315	Esi 4/72	Esc 1/8	Fso 5/53	Fsi 3/20	Fsc 1/3	Hsx 21/3076
Cao 34/1282	Cai 2/27	Dao 91/2081	Dai 48/466	Dac 21/68	Eao 50/587	Eai 60/454	Eac 11/76	Fao 10/100	Fai 24/143	Fac 8/31	Hax 10/867
Cho 2/81	Chi 0/3	Dho 3/57	Dhi 0/12	Dhc 1/5	Eho 2/33	Ehi 7/30	Ehc 0/4	Fho 3/19	Fhi 2/10	Fhc 10/10	Hhx 2/102
Cko 12/139	Cki 1/8	Dko 31/187	Dki 38/178	Dkc 51/107	Eko 25/155	Eki 65/326	Ekc 119/230	Fko 13/70	Fki 74/184	Fkc 200/222	Hkx 3/101

number of events occurring in a fixed interval of time or space if these events occur with a known mean flare occurrence rate independent of the time since the last events.

The flare probability of observing N events per unit time interval is given by the Poisson distribution:

$$P_{\mu}(N) = \frac{\mu^N}{N!} \exp(-\mu), \quad (1)$$

where μ is the flare occurrence rate expected in each time interval. The probability of observing one or more flares in a 24 h period can then be estimated by

$$P_{\mu}(N \geq 1) = 1 - P_{\mu}(N = 0), \quad (2)$$

where $P_{\mu}(N = 0)$ is the probability of no flares occurring. Certainly, the probability is given by

$$P_{\mu}(N \geq 1) = 1 - \exp(-\mu). \quad (3)$$

Thus, for the 'Fkc' region with an flare occurrence rate of 2.39, the probability for one or more C-class flares to occur in a given 24 h period is

$$\begin{aligned} P_{\mu=2.39}(N \geq 1) &= 1 - \exp(-2.39) \\ &= 0.9. \end{aligned} \quad (4)$$

In order to estimate the flare probability, we apply this methodology to each sub-group: "Large", "Small", "Decrease", "Steady", and "Increase".

3. Results

We have estimated the probability and occurrence rate of flares in terms of the sunspot classification supplemented with sunspot area and its changes. We will present our results in the forms of graphs and tables.

3.1. Flare Occurrence Rate and Probability in Terms of the Sunspot Classification Supplemented with Sunspot Area

The mean flare occurrence rates in terms of sunspot classification supplemented with sunspot area are shown in Figure 1 for the C-class flares and in Figure 2 for the (M + X)-class flares. The flare occurrence rates in the "Large" sub-groups are higher than those in the "Small" sub-groups; 30–50 % enhancement for the C-class flares and 30–120 % enhancement for the (M + X)-class flares. Especially in the 'Dkc', 'Ekc', 'Fki', and 'Fkc' sunspot groups, the occurrence rates of the (M + X)-class flares in the "Large" sub-groups are about two times higher than those in the "Small" sub-groups. In the case of the "Large" sub-group of the 'Fkc' sunspot group, the flare occurrence rate is higher than one, implying that major flares occur more than once in a day on average. The flare occurrence rates of two sub-groups ("Large" and "Small") for the 'Dai', 'Eai', 'Dko', and 'Dki' groups are similar to each other. The flare occurrence rates and probabilities thus derived are tabulated in Table 3 for the C-class flares and Table 4 for the (M + X)-class flares.

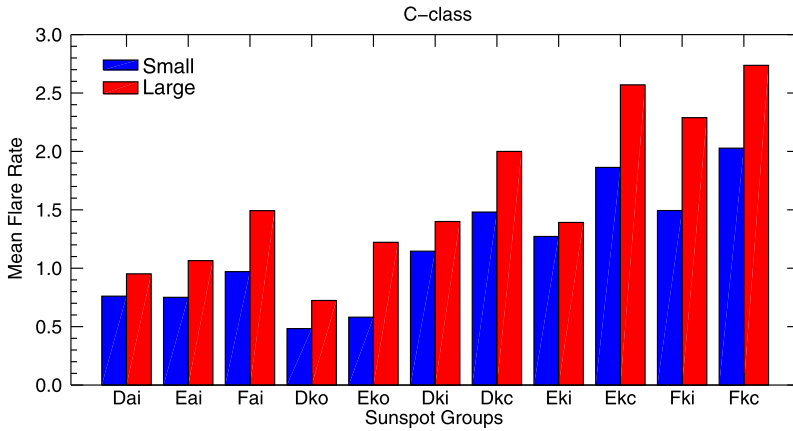


Figure 1 Flare occurrence rates in terms of the sunspot classification supplemented with sunspot area in case of C-class flares. The red and blue bars show the “Large” and “Small” sub-groups, respectively.

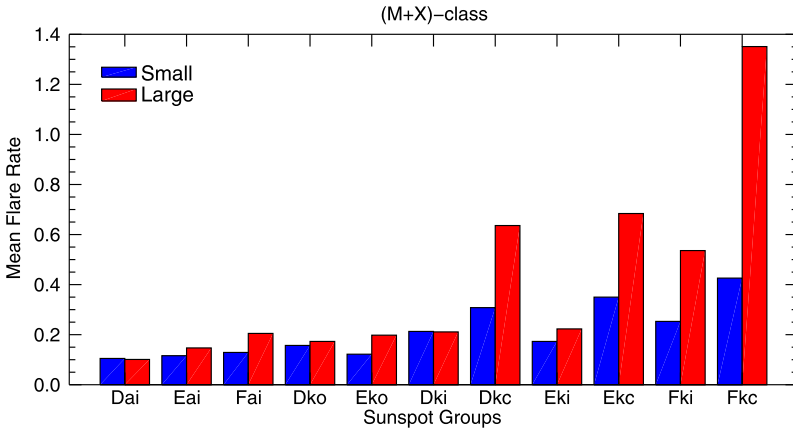


Figure 2 Flare occurrence rates in terms of the sunspot classification supplemented with sunspot area in case of (M + X)-class flares. The red and blue bars show the “Large” and “Small” sub-groups, respectively.

3.2. Flare Occurrence Rate and Probability in Terms of the Sunspot Classification Supplemented with Sunspot Area Changes

We next investigate the relationship between the flare occurrence rate and sunspot classes supplemented with sunspot area changes. The results are plotted in Figure 3 for the C-class flares and in Figure 4 for the (M + X)-class flares, respectively. For most cases, the flare occurrence rates of “Increase” sub-groups are larger than those of the other sub-groups. In case of the C-class flares, the flare occurrence rates of the “Increase” sub-group in the ‘Dai’, ‘Fai’, ‘Dkc’, and ‘Ekc’ groups are noticeably higher than those of the other sub-groups. In case of the (M + X)-class flares, the flare occurrence rates of the “Increase” sub-groups in ‘Fai’, ‘Dko’, and ‘Dkc’ sunspot groups are three times higher than those of the “Steady” sub-groups. The flare occurrence rates and flare probabilities are summarized in Table 5 for the C-class flares and in Table 6 for the (M + X)-class flares.

Table 3 Flare occurrence rates and probabilities in terms of the sunspot classification supplemented with sunspot area, in the case of C-class flares.

Class	Mean flare rate		Probability (%)	
	Small	Large	Small	Large
Dai	0.76	0.95	53	61
Eai	0.75	1.07	53	66
Fai	0.97	1.49	62	78
Dko	0.48	0.72	38	52
Eko	0.58	1.22	44	71
Dki	1.15	1.39	68	75
Dkc	1.48	2.00	77	86
Eki	1.27	1.39	72	75
Ekc	1.86	2.57	85	92
Fki	1.49	2.29	78	90
Fkc	2.03	2.74	86	94

Table 4 Flare occurrence rates and probabilities in terms of the sunspot classification supplemented with sunspot area, in the case of (M + X)-class flares.

Class	Mean flare rate		Probability (%)	
	Small	Large	Small	Large
Dai	0.11	0.10	10	10
Eai	0.12	0.15	11	14
Fai	0.13	0.21	12	19
Dko	0.16	0.17	15	16
Eko	0.12	0.20	12	18
Dki	0.21	0.21	19	19
Dkc	0.31	0.64	26	47
Eki	0.17	0.22	16	20
Ekc	0.35	0.68	30	50
Fki	0.25	0.54	22	41
Fkc	0.43	1.35	35	74

4. Summary and Conclusions

In this study, we have examined the occurrence rate and probability of flares in terms of our sunspot classification which is supplemented with sunspot area and its changes. For this we used sunspot data from 1996 to 2010. We noted that sunspot area and its changes can be a proxy of magnetic flux and its emergence/cancellation, respectively. We classify each sunspot group into the following sub-groups: “Large” and “Small” according to its area and “Decrease”, “Steady”, and “Increase” according to its area changes. Major results from this study can be summarized as follows.

- i) In the McIntosh sunspot group classification (60 classes in total), the most flare-productive 11 sunspot groups are ‘Dai’, ‘Eai’, ‘Fai’, ‘Dko’, ‘Eko’, ‘Dki’, ‘Dkc’, ‘Eki’, ‘Ekc’, ‘Fki’, and ‘Fkc’.
- ii) In case of large and compact groups, the flare probabilities noticeably increase with sunspot area.
- iii) When the sunspot area increases, the flare occurrence rates and probabilities noticeably increase, especially for major flares.

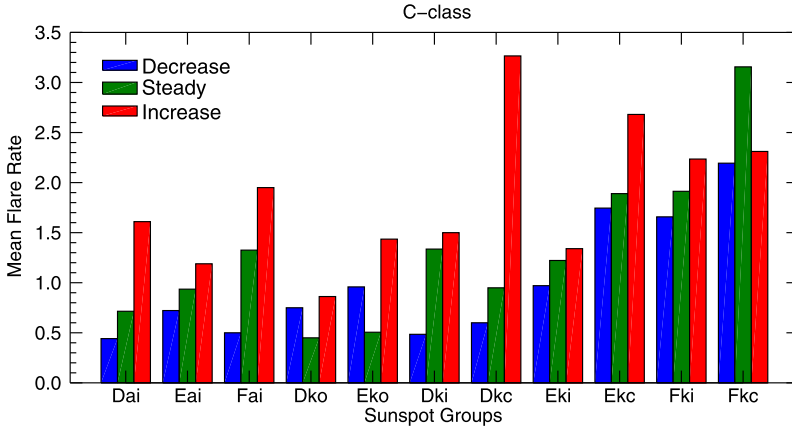


Figure 3 Flare occurrence rates in terms of the sunspot classification supplemented with sunspot area changes in the case of C-class flares. The blue, green, and red bars show the “Decrease”, “Steady”, and “Increase” sub-groups, respectively.

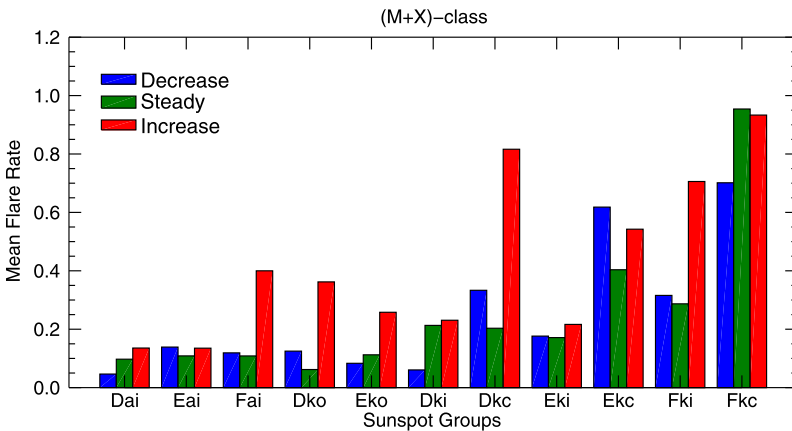


Figure 4 Flare occurrence rates in terms of the sunspot classification supplemented with sunspot area changes in the case of (M + X)-class flares. The blue, green, and red bars show the “Decrease”, “Steady”, and “Increase” sub-groups, respectively.

We consider the most flare-productive 11 sunspot group classes: ‘Dai’, ‘Eai’, ‘Fai’, ‘Dko’, ‘Eko’, ‘Dki’, ‘Dkc’, ‘Eki’, ‘Ekc’, ‘Fki’, and ‘Fkc’. We compare the flare occurrence rates with other results reported by Kildahl (1980) for 1969–1976 and Norquist (2011) for 2000–2007. Our results show that the sunspot classes having the top five flare occurrence rates are ‘Fkc’, ‘Ekc’, ‘Dkc’, ‘Fki’, and ‘Eki’, which is a little different from Kildahl’s (1980) results (‘Ekc’, ‘Fki’, ‘Fkc’, ‘Eki’, and ‘Dkc’) and from Norquist’s (2011) results (‘Fkc’, ‘Ekc’, ‘Fac’, ‘Eki’, and ‘Fko’). Such differences may be due to different observing periods and different versions of the McIntosh classification; for example, while Kildahl (1980) used 63 classification types, the present study uses 60 classification types. We note that ‘Fkc’ and ‘Ekc’ sunspot groups are included in all three studies. This fact may imply that large, asymmetric penumbra sunspot groups should be most flare productive.

Table 5 Flare occurrence rates and probabilities in terms of the sunspot classification supplemented with sunspot area changes, in the case of C-class flares.

Class	Mean flare rate			Probability (%)		
	Decrease	Steady	Increase	Decrease	Steady	Increase
Dai	0.44	0.75	1.61	36	51	80
Eai	0.72	0.94	1.19	51	61	70
Fai	0.50	1.33	1.95	39	73	86
Dko	0.75	0.45	0.86	53	36	58
Eko	0.96	0.51	1.44	62	40	76
Dki	0.48	1.34	1.50	38	74	78
Dkc	0.60	0.95	3.27	45	61	96
Eki	0.97	1.22	1.34	62	71	74
Ekc	1.75	1.89	2.68	83	85	89
Fki	1.66	1.91	2.24	81	85	89
Fkc	2.19	3.16	2.31	89	96	90

Table 6 Flare occurrence rates and probabilities in terms of the sunspot classification supplemented with sunspot area changes, in the case of (M + X)-class flares.

Class	Mean flare rate			Probability (%)		
	Decrease	Steady	Increase	Decrease	Steady	Increase
Dai	0.05	0.10	0.14	5	9	13
Eai	0.14	0.11	0.14	13	10	13
Fai	0.12	0.11	0.40	11	10	33
Dko	0.13	0.06	0.36	12	6	30
Eko	0.08	0.11	0.26	8	11	23
Dki	0.06	0.21	0.23	6	19	21
Dkc	0.33	0.20	0.82	28	18	56
Eki	0.18	0.17	0.22	16	16	19
Ekc	0.62	0.40	0.54	46	33	42
Fki	0.32	0.29	0.71	27	25	51
Fkc	0.70	0.95	0.93	50	61	61

From the relationship between flare probability and sunspot group area, in the case of large and compact groups, the solar flare probabilities are higher than those of other groups. Especially, ‘Dkc’, ‘Ekc’, and ‘Fkc’ sunspot groups are most flare-productive groups, which is consistent with McIntosh (1990) who suggested that flares prefer the larger and more complex sunspot groups. Bornmann and Shaw (1994) and Sammis, Tang, and Zirin (2000) also showed that larger and more complex regions produce more numerous and larger flares.

In the case of “Increase” sub-groups, the flare occurrence rates and probabilities are higher than other sub-groups. This means that when the sunspot area is larger, then the flare probability becomes higher. This is statistical evidence that magnetic flux emergence is an important mechanism for triggering solar flares, because sunspot area can be a good proxy of magnetic flux (Zharkov and Zharkova, 2006).

Table 7 Mean flare occurrence rates and probabilities for all sunspot groups.

Class	Mean flare rate		Probability (%)	
	C-class	(M + X)-class	C-class	(M + X)-class
Decrease	1.00	0.24	58	20
Steady	1.31	0.25	67	20
Increase	1.85	0.43	96	33

It is worthwhile to see the overall tendency in flare occurrence rates among the sub-groups representing sunspot area changes. To do this, we calculate the average of flare occurrence rates and probabilities for each sub-group. Table 7 shows that mean flare occurrence rates and probabilities for all sunspot groups increase with the following order: “Decrease”, “Steady”, and “Increase”. Our results statistically demonstrate that magnetic flux and its emergence enhance major solar flare occurrence. Finally, our results can be used for improving solar flare prediction models.

Acknowledgements This work has been supported by the WCU program (No. R31-10016) through the National Research Foundation of Korea funded by the Ministry of Education, Science and Technology and by the Korea Research Foundation Grant funded by the Korean Government (MOEHRD, Basic Research Promotion Fund) (20090071744 and 20100014501), and the Korea Meteorological Administration/National Meteorological Satellite Center.

References

- Andrews, M.D.: 2003, *Solar Phys.* **218**, 261.
- Baker, D.N.: 2005, In: Scherer, K., Fichtner, H., Heber, B., Mall, U. (eds.) *Space Weather – The Physics Behind a Slogan, Lecture Notes in Physics* **656**, Springer, Berlin, 3.
- Barnes, G., Leka, K.D., Schumer, E.A., Della-Rose, D.J.: 2007, *Space Weather* **5**, S09002.
- Borrmann, P.L., Kalmbach, D., Kulhanek, D.: 1994, *Solar Phys.* **150**, 147.
- Borrmann, P.L., Shaw, D.: 1994, *Solar Phys.* **150**, 127.
- Colak, T., Qahwaji, R.: 2008, *Solar Phys.* **248**, 277.
- Cortie, A.L.: 1901, *Astrophys. J.* **13**, 260.
- Gallagher, P.T., Moon, Y.-J., Wang, H.: 2002, *Solar Phys.* **209**, 171.
- Giovanelli, R.G.: 1939, *Astrophys. J.* **89**, 555.
- Greatix, G.R.: 1963, *Mon. Not. Roy. Astron. Soc.* **126**, 132.
- Hale, G.E., Ellerman, F., Nicholson, S.B., Joy, A.H.: 1919, *Astrophys. J.* **49**, 153.
- Heyvaerts, J., Priest, E.R., Rust, D.M.: 1977, *Astrophys. J. Lett.* **216**, L123.
- Kildahl, K.: 1980, In: Donnelly, F.F. (ed.) *Solar-Terrestrial Predictions Proceedings* **3**, U.S. Dept. Commerce, Boulder, 166.
- McIntosh, P.S.: 1990, *Solar Phys.* **125**, 251.
- Moon, Y.-J., Choe, G.S., Yun, H.S., Park, Y.D.: 2001, *J. Geophys. Res.* **106**, 29951.
- Norquist, D.C.: 2011, *Solar Phys.* **269**, 111.
- Sammis, I., Tang, F., Zirin, H.: 2000, *Astrophys. J.* **540**, 583.
- Tur, T.J., Priest, E.R.: 1978, *Solar Phys.* **58**, 181.
- Veronig, A.M., Temmer, M., Hanslmeier, A.: 2004, *Solar Phys.* **219**, 125.
- Walmeier, M.: 1947, *Publ. Zür. Obs.* **9**, 1.
- Wheatland, M.S.: 2000, *Astrophys. J. Lett.* **536**, L109.
- Wheatland, M.S.: 2004, *Astrophys. J. Lett.* **609**, L1134.
- Wheatland, M.S.: 2005, *Space Weather* **3**, S07003.
- Wang, H.N., Cui, Y.M., Li, R., Zhang, L.Y., Han, H.: 2008, *Adv. Space Res.* **42**, 1464.
- Yu, D.R., Huang, X., Wang, H.N., Cui, Y.M.: 2009, *Solar Phys.* **255**, 91.
- Yuan, Y., Shih, F.Y., Jing, J., Wang, H.: 2010, *Res. Astron. Astrophys.* **10**, 785.
- Zharkov, S.I., Zharkova, V.V.: 2004, In: Stepanov, A.V., Benevolenskaya, E.E., Kosovichev, A.G. (eds.) *Multi-Wavelength Investigations of Solar Activity, IAU Symp.* **223**, 711.
- Zharkov, S.I., Zharkova, V.V.: 2006, *Adv. Space Res.* **38**, 868.